



Title	The role of artificial defects for engineering large effective mode area, flat chromatic dispersion, and low leakage losses in photonic crystal fibers: Towards high speed reconfigurable transmission platforms
Author(s)	Florous, Nikolaos; Saitoh, Kunimasa; Koshiba, Masanori
Citation	Optics Express, 14(2), 901-913 https://doi.org/10.1364/OPEX.14.000901
Issue Date	2006-01
Doc URL	http://hdl.handle.net/2115/5418
Rights	© 2006 Optical Society of America, Inc.
Type	article (author version)
File Information	OE14-2006.pdf



[Instructions for use](#)

The role of artificial defects for engineering large effective mode area, flat chromatic dispersion, and low leakage losses in photonic crystal fibers: Towards high speed reconfigurable transmission platforms

Nikolaos Florous, Kunimasa Saitoh, and Masanori Koshiba

Division of Media and Network Technologies, Hokkaido University, Sapporo 060-0814, Japan
nflorous@dpo7.ice.eng.hokudai.ac.jp

Abstract: The present paper describes a novel systematic solution to the challenging task of realizing photonic crystal fibers (PCFs) with flat chromatic dispersion, low leakage losses, and large mode area, mainly for applications as information carriers in wide-band high speed optical transmission systems. The proposed design strategy is based on the existence of an artificially-defected air-hole ring in the cladding and on the modulation of the refractive index of the core by assembling additional defected air-holes in the central core region of the fiber. The validation of the proposed design is carried out by adopting an efficient full-vectorial finite element method with perfectly matched layers for accurate characterization of PCFs. The remarkable flat chromatic dispersion as well as the large mode area and the low leakage losses are the main advantages of the proposed PCF structure, making it an ideal candidate for performing wavelength division multiplexing operation in reconfigurable optical transmission systems or as an information delivering platform in high speed optical communication systems. Typical characteristics of the newly proposed PCF are: flattened chromatic dispersion of 6.3 ± 0.5 ps/km/nm in the S+C+L telecommunication band, and effective mode area as large as $100 \mu\text{m}^2$ in the same wavelength range. We additionally provide numerical data about the performance of the proposed PCF in splicing mode as well as during macrobending operation and we give qualitative information regarding the sensitivity of the proposed transmission platform to structural disorders of the design parameters.

©2005 Optical Society of America

OCIS codes: (060.2430) Fibers, single mode; (999.9999) Photonic crystal fiber

References and links

1. J. A. Buck, *Fundamentals of Optical Fibers*, Wiley-Interscience (2004).
2. J. C. Knight, "Photonic crystal fibers," *Nature* **424**, 847-851 (2003).
3. J. C. Knight, T. A. Birks, P. St. J. Russel, and D. M. Atkin, "All-silica single-mode optical fiber with photonic crystal cladding," *Opt. Lett.* **21**, 484-485 (1996).
4. M. D. Nielsen, C. Jacobsen, N. A. Mortensen, J. R. Folkenberg, and H. R. Simonsen, "Low-loss photonic crystal fibers for transmission system and their dispersion properties," *Opt. Express* **12**, 1372-1376 (2004), <http://www.opticsexpress.org/abstract.cfm?URI=OPEX-11-24-1372>.
5. K. Saitoh, M. Koshiba, T. Hasegawa, and E. Sasaoka, "Chromatic dispersion control in photonic crystal fibers: application to ultra-flattened dispersion," *Opt. Express* **11**, 843-852 (2003), <http://www.opticsexpress.org/abstract.cfm?URI=OPEX-11-08-843>.
6. J. Zhou, K. Tajima, K. Nakajima, K. Kurokawa, C. Fukai, T. Matsui, and I. Sankawa, "Progress on low loss photonic crystal fibers," *Opt. Fiber Technol.* **11**, 101-106 (2005).

7. K. Tajima, J. Zhou, K. Nakajima, and K. Sato, "Ultralow loss and long length photonic crystal fiber," *J. Lightwave Technol.* **22**, 7-10 (2004).
8. K. Nakajima, J. Zhou, K. Tajima, K. Kurokawa, C. Fukai, and I. Sankawa, "Ultrawid-band single-mode transmission performance in a low-loss photonic crystal fiber," *J. Lightwave Technol.* **23**, 7-12 (2005).
9. A. Ferrando, E. Silvestre, P. Andres, J. J. Miret, and M. V. Andres, "Designing the properties of dispersion-flattened photonic crystal fibers," *Opt. Express* **9**, 687-697 (2001), <http://www.opticsexpress.org/abstract.cfm?URI=OPEX-9-13-687>.
10. T. Yamamoto, H. Kubota, S. Kawanishi, M. Tanaka, and S. Yamaguchi, "Supercontinuum generation at 1.55 μm in a dispersion-flattened polarization-maintaining photonic crystal fiber," *Opt. Express* **11**, 1537-1540 (2003), <http://www.opticsinfobase.org/abstract.cfm?URI=oe-11-13-1537>.
11. K. Saitoh and M. Koshiba, "Highly nonlinear dispersion-flattened photonic crystal fibers for supercontinuum generation in a telecommunication window," *Opt. Express* **12**, 2027-2032 (2004), <http://www.opticsexpress.org/abstract.cfm?URI=OPEX-12-10-2027>.
12. K. Saitoh, N. Florous, and M. Koshiba, "Ultra-flattened chromatic dispersion controllability using a defected-core photonic crystal fiber with low confinement losses," *Opt. Express* **13**, 8365-8371 (2005) <http://www.opticsinfobase.org/abstract.cfm?URI=oe-13-21-8365>.
13. A. Belahlou, S. Bickham, D. Chowdhury, P.D.A. Evans, J.M. Grochocinski, P. Han, A. Kobaykov, S. Kumar, G. Lutter, J.C. Mauro, Y. Mauro, M. Mlejnek, M.S.K. Muktoyuk, M.T. Murtagh, S. Raghavan, V.R.A. Sevian, N.Taylor, S. Tsuda, M. Vasilyev, and L. Wang, "Fiber design considerations for 40 Gb/s systems," *J. Lightwave Technol.* **20**, 2290-2305 (2002).
14. K. Saitoh and M. Koshiba, "Full-vectorial imaginary-distance beam propagation method based on a finite element scheme: application to photonic crystal fibers," *IEEE J. Quantum Electron.* **38**, 927-933 (2002).
15. K. Mukasa, F. Poletti, K. Imamura, N. Kumano, T. Yagi, and D.J. Richardson, "A high performance $\text{GeO}_2/\text{SiO}_2$ NZ-DSF and the prospects for future improvements using Holey Fiber technology," in proceedings of European Conference on Optical Communications (ECOC2005), paper Tu1.4.6, Glasgow, Scotland, (2005).
16. D. Davidson, *Optical-Fiber Transmission* (E. E. Bert Basch , ed., Howard W. Sams & Co, 1987).
17. Y. Tsuchida, K. Saitoh, and M. Koshiba, "Design and characterization of single-mode holey fibers with low bending losses," *Opt. Express* **13**, 4770-4779 (2005), <http://www.opticsexpress.org/abstract.cfm?URI=OPEX-13-12-4770>.
18. M. Koshiba, H. Saitoh, M. Eguchi, and K. Hirayama, "A simple scalar finite element approach to optical rib waveguide," *IEE Proc. Part J: Optoelectron.* **139**, 166-171 (1992).
19. J. C. Knight, T. A. Birks, P. St J. Russell, and J. P. de Sandro, "Properties of photonic crystal fiber and the effective index model," *Opt. Lett.* **15**, 748-752 (1998).
20. F. Poletti, V. Finazzi, T. M. Monro, N. G. R. Broderick, V. Tse, and D. J. Richardson, "Inverse design and fabrication tolerances of ultra-flattened dispersion holey fibers," *Opt. Express* **13**, 3728-3736 (2005), <http://www.opticsexpress.org/abstract.cfm?URI=OPEX-13-10-3728>.

1. Introduction

Optical fibers which can transmit the information in the form of short optical pulses over long distances have revolutionized telecommunication industry in the last two decades [1]. In particular the propagation of light-waves in periodic and disordered dielectric systems has attracted considerably attention in recent years and as a result of extensive studies performed by many researchers all around the world, a new class of optical fibers that enables light to be controlled in ways not previously possible or even imaginable has emerged, known as photonic crystal fiber (PCF) [2]. As a result of their extra ordinary properties, PCFs have become a pre-eminent method for transmitting information and realizing optical devices [3].

Index-guiding PCFs, also known as holey fibers have particularly attracted considerably attention from the optical scientific community. One of the appealing properties of PCFs is the fact that they can possess dispersion properties significantly different than those of the conventional optical fibers, because their artificially-periodic cladding consisting of micrometer-sized air-holes, allows the flexible tailoring of the dispersion curves. The task of controlling the chromatic dispersion is a very important problem in designing practical optical communication systems [4], as well as dispersion controllers [5].

As the attenuation of index-guiding PCFs has been constantly reduced up to a level of 0.28 dB/km at 1.55 μm wavelength [6], a great vision regarding the use of PCFs has emerged, that is apart of realizing optical components, as platforms for transmitting information [4,7,8] especially in wide-band high speed transmission systems. In such a case, both the

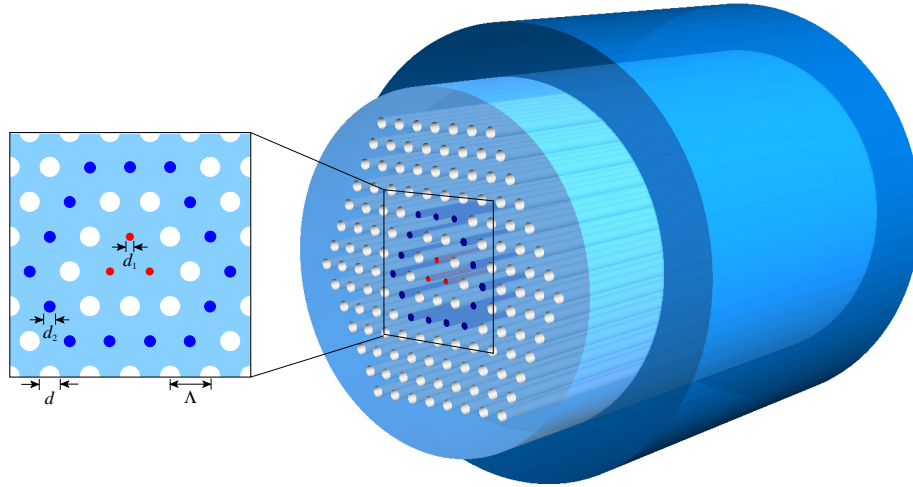


Fig. 1. Schematic representation of the proposed PCF structure. The air-holes in the cladding are arranged in a triangular configuration with lattice constant Λ and air-hole diameters- d . The central core is perturbed with three extra air-holes (red colored circles) with reduced in size diameters- d_1 positioned in the core-region. An artificially defected air-hole ring with reduced air-hole diameters- d_2 (blue colored circles) is assembled in the cladding. By a judicious choice of the geometrical parameters, this PCF structure can exhibit flat chromatic dispersion with large mode area and low confinement losses.

controllability of the chromatic dispersion, and the enlargement of the effective mode area are very crucial factors in terms of the quality of information transmission.

So far various types of PCFs with remarkable chromatic dispersion characteristics have been reported in the international literature [9-12]. To the best of our knowledge however, the task to engineer dispersion flattened PCFs with large mode area and low leakage losses at the same time, particularly useful in designing high speed communication systems based on wavelength division multiplexing [13] has not been reported so far. Since such a class of PCFs will be an important break-through in realizing modern reconfigurable optical communication systems, we therefore devote the present paper to describe an intriguing design approach for realizing a novel type of PCF having all the above mentioned characteristics, that is ultra-flattened chromatic dispersion, large mode area as well as low leakage losses. The basic idea for achieving all the above mentioned propagation characteristics of the newly proposed PCF is based on the presence of an artificially-defected air-hole ring in the cladding of the PCF for enlarging the effective mode area and on the modulation of the core's effective index with the inclusion of additional defected air-holes in the center of the fiber for the dynamic controllability of the chromatic dispersion. To validate the design we perform extensive numerical simulations using a full-vectorial finite element method (FEM) [14], with hybrid edge/nodal elements and anisotropic perfectly matched layers for accurate modeling of PCFs. Our proposed design shows better performance in comparison to conventional large mode area non-zero dispersion shifted fiber with low dispersion slope [15]. The composition of the present study will be as follows: In Section 2 we introduce the proposed PCF topology and we give a priori detailed design guidelines for achieving the desired performance. Then in Section 3 we present quantitative numerical results for validating our design. To justify the use of the proposed topology in transmission systems in Section 4 we study the single mode operation and the confinement loss properties and we address possible issues regarding additional loss mechanisms in this new type of PCF. Then in Section 5 we briefly discuss the feasibility and the compatibility of the proposed PCF with other conventional optical fibers by presenting results on macro-bending as well as splice

losses. In order to identify possible flaws during the fabrication process of the proposed PCF structure in Section 6 we present qualitative numerical data regarding sensitivity analysis of various quantities to structural disorders of the design parameters. Finally in Section 7 we conclude our work and we give some possible directions for further investigations.

2. Schematic cross section and design guidelines of the proposed PCF

Consider the schematic cross section of the PCF structure as shown in Fig. 1. It is composed of circular air-holes in the cladding arranged in a triangular array with lattice constant Λ and diameters- d . The host material is pure silica. The central core area of the fiber has been perturbed to have nearly triangular shape, while it has also been modulated by embedding three extra air-holes with reduced in size diameters- d_1 whose function is the controllability of the chromatic dispersion as it will be demonstrated later on. The core region therefore has an area as large as that of three unit cells, where the unit cell is defined the same way as in regular photonic crystal structures. The inclusion of an artificially-defected air-hole ring in the cladding of the fiber with reduced in size diameters- d_2 has the function to enlarge the mode area without destroying the flattened chromatic dispersion. To accurately predict the propagation properties of this PCF structure we have adopted an efficient FEM modal solver [14] with curvilinear edge/nodal hybrid elements in order to predict with high accuracy all the propagation properties of this PCF.

The following observations will define the design strategy for achieving the flat dispersion characteristics for this type of PCF. It is well known fact that a PCF possesses great controllability of the chromatic dispersion in comparison with the conventional optical cables. In conventional PCFs, the chromatic dispersion profile can be easily altered by varying the size of the air-hole diameters and the lattice constant. When the air-hole diameters are relatively large and the lattice constant is small, the influence of the waveguide dispersion in the fiber becomes stronger, and unusual dispersion characteristics can be achieved. On the other hand, as the air-hole diameters are decreasing and the lattice constant increases, the total chromatic dispersion curve comes closer to the material dispersion of pure-silica, because the core region in typical PCFs is a solid composition of silica. Therefore by using a conventional type of PCF topology it is difficult to engineer the ultra-flattened chromatic dispersion and the large mode area at the same time. As a consequence we need to incorporate a much more sophisticated structure with more degrees of freedom regarding the total number of design parameters in order to achieve having flat dispersion and large mode area, while keeping the confinement losses as low as possible. The proposed PCF in Fig. 1 is an ideal candidate for our design purpose, since the absence of a totally solid core-region will automatically generate a remarkable wavelength-dependence of the effective refractive index of the core. This strong wavelength-dependence is the key factor which will lead to the controllability of the chromatic dispersion of the fiber, by adjusting the size of the defected air-hole diameters- d_1 , while the incorporation of a defected air-hole ring at the cladding will enlarge the effective mode area with a result of improving the quality of the signal transmittivity through this PCF structure.

3. Numerical results and performance verification of the proposed PCF topology

To succeed obtaining nearly-zero total chromatic dispersion, we can see that if we are able to design the proposed PCF in such a way that can exhibit waveguide dispersion $D_w(\lambda)$ nearly opposite to that of the material dispersion $D_m(\lambda)$, namely $D_w(\lambda) \cong -D_m(\lambda)$ over a continuous spectral range [9,16], we can partially fulfill the nearly-zero dispersion requirement. To show the impact of the variation of the design parameter- d_1 to the chromatic dispersion curve, in Fig. 2 we plot the normalized waveguide dispersion (colored curves) of the proposed PCF as a function of the normalized wavelength λ/Λ , for various incremental values of the normalized

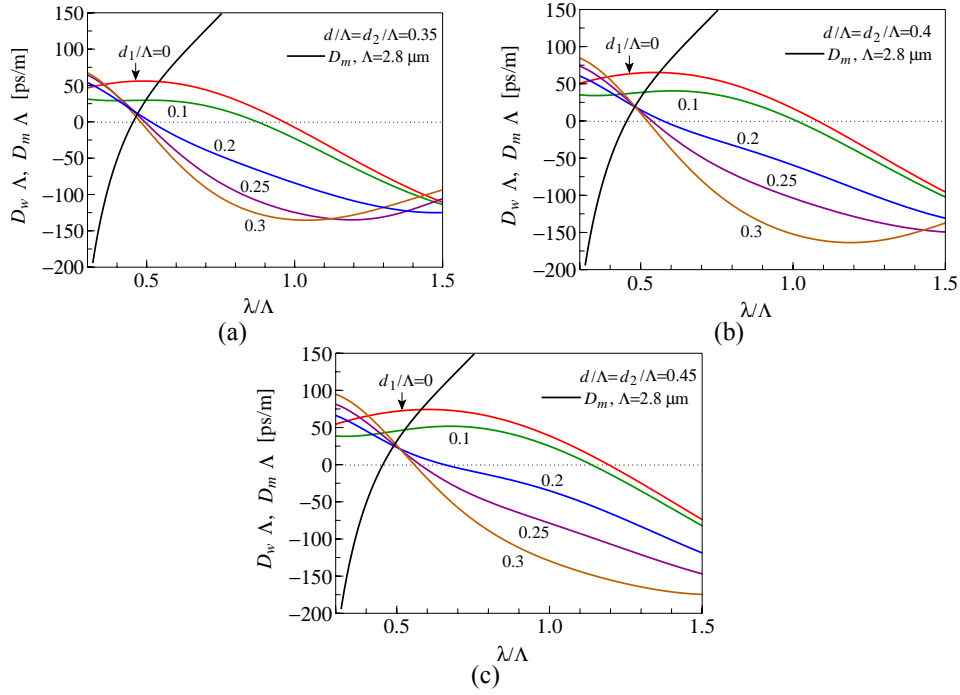


Fig. 2. Normalized waveguide dispersion curves $D_w\Lambda$ as a function of the normalized wavelength λ/Λ , for various incremental values of the design parameter d_1/Λ , specifically $d_1/\Lambda=0$ (red curve), $d_1/\Lambda = 0.1$ (green curve), $d_1/\Lambda = 0.2$ (blue curve), $d_1/\Lambda = 0.25$ (purple curve), and $d_1/\Lambda = 0.3$ (orange curve), for (a) fixed air-hole diameters in the cladding $d/\Lambda = d_2/\Lambda=0.35$, (b) fixed air-hole diameters in the cladding $d/\Lambda = d_2/\Lambda=0.4$, and (c) fixed air-hole diameters in the cladding $d/\Lambda = d_2/\Lambda=0.45$. The black curve in all cases represents the normalized material dispersion of silica $D_m\Lambda$ at a fixed lattice constant of $\Lambda = 2.8 \mu\text{m}$.

design parameter d_1/Λ , for (a) uniformly fixed parameters $d/\Lambda=d_2/\Lambda=0.35$, (b) uniformly fixed parameters $d/\Lambda=d_2/\Lambda=0.4$, and (c) uniformly fixed parameters $d/\Lambda=d_2/\Lambda=0.45$, while the silica index is assumed equal to 1.45 for calculating the waveguide dispersion. The black curve represents the material dispersion in all graphs, which has been calculated using the Sellmeier's equation, assuming the lattice constant fixed to the value of $\Lambda=2.8 \mu\text{m}$. From the results in Fig. 2 we can observe that by increasing the value of the design parameter- d_1 the waveguide dispersion decreases. Eventually there will be a value of d_1 such that the waveguide dispersion curve in all cases will become nearly anti-symmetric to that of the material dispersion, namely $D_w(\lambda)\cong -D_m(\lambda)$ and thus we can fulfill the requirement for flat dispersion. The approximate value in such a case is $d_1/\Lambda=0.28$ at fixed lattice constant of $\Lambda=2.8 \mu\text{m}$ and $d/\Lambda=0.35$, while for $d/\Lambda=0.4$ the approximate value has been determined to be $d_1/\Lambda=0.29$ and for $d/\Lambda=0.45$ it has been determined to be $d_1/\Lambda=0.30$.

Having obtained the desired flat chromatic dispersion characteristics, next we consider how to realize the large mode area. With a micro-adjustment of the design parameter- d_2 we can successfully enlarge the effective mode area to a desired value. In order to show the impact of the design parameter- d_2 of the defected ring to the chromatic dispersion and to the effective mode area, in Fig. 3 we plot the total chromatic dispersion (i.e. including the material dispersion in the calculations) and its corresponding effective mode areas. Particularly Fig. 3(a) shows the tendency of the chromatic dispersion curves as a function of the wavelength λ for different values of the design parameter d_2/Λ , with the other design

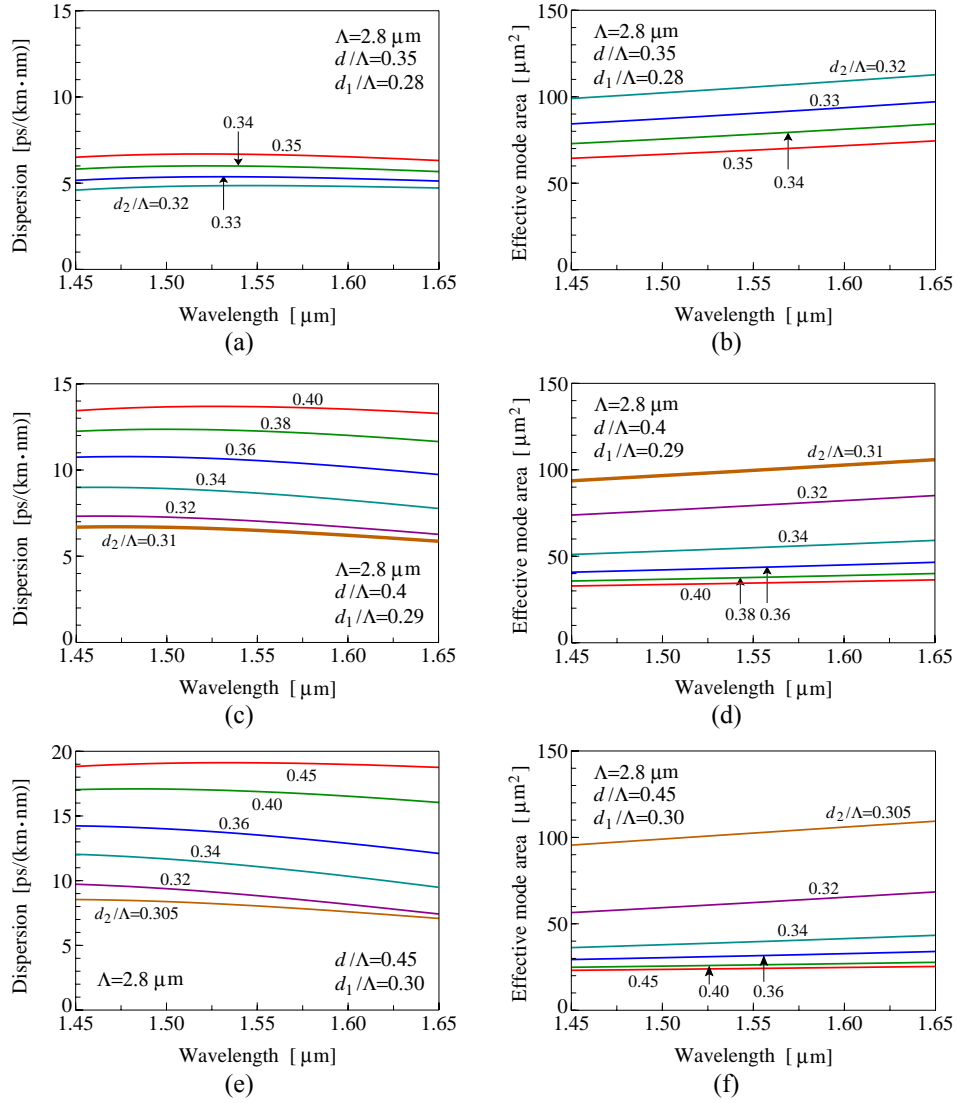


Fig. 3. (a) Total chromatic dispersion curves as a function of the wavelength- λ , for different values of the design parameter- d_2/Λ , for fixed air-hole diameters in the cladding $d/\Lambda=0.35$ and fixed defected air-holes in the core $d_1/\Lambda=0.28$, (b) the corresponding effective mode areas, (c) total chromatic dispersion curves as a function of the wavelength- λ , for different values of the design parameter- d_2/Λ , for fixed air-hole diameters in the cladding $d/\Lambda=0.4$ and fixed defected air-holes in the core $d_1/\Lambda=0.29$, (d) the corresponding effective mode areas, (e) total chromatic dispersion curves as a function of the wavelength- λ , for different values of the design parameter- d_2/Λ , for fixed air-hole diameters in the cladding $d/\Lambda=0.45$ and fixed defected air-holes in the core $d_1/\Lambda=0.3$, (f) the corresponding effective mode areas. It is evident that for the three different groups of design parameters the continuous decrement of the design parameter- d_2 will result in the continuous increment of the effective mode area while the chromatic dispersion will continuously decrease, while keeping its flatness.

parameters fixed at values of $d/\Lambda=0.35$, $d_1/\Lambda=0.28$, $\Lambda=2.8 \mu\text{m}$, considering in total 11 air-hole rings in the PCF, while in Fig. 3(b) we plot the corresponding effective mode areas. The same is repeated in Fig. 3(c) for the chromatic dispersion but for different fixed set of design

parameters, that is $d/\Lambda=0.4$, $d_1/\Lambda=0.29$, and $\Lambda=2.8\ \mu\text{m}$, while Fig 3(d) shows the corresponding effective mode areas for the same set of design parameters as in Fig. 3(c). In Fig. 3(e) we show the calculated dispersion curves for a different set of design parameters, that is for $d/\Lambda=0.45$, $d_1/\Lambda=0.3$, and $\Lambda=2.8\ \mu\text{m}$, and for different values of the design parameter d_2/Λ , while in Fig. 3(f) we plot the corresponding effective mode areas for this set of design parameters. Notice that the results concerning the chromatic dispersion in all cases have been obtained using the knowledge of the effective index of the fundamental mode including the wavelength-dependence of pure silica in the FEM modal solver. From the results in Figs. 3(a), (c) and (e) we may observe that by decreasing the size of the air-holes in the artificially-defected air-hole ring, the chromatic dispersion decreases, but without destroying the flatness. The thick orange curves in Figs. 3(c) and (d) correspond to the optimum selection of the design parameters as it will be explained later on. In Figs. 3(b), (d), and (f) we can examine what happens to the effective mode area. From these results we can clearly see that the continuous decrement of the design parameter- d_2 results in the continuous increment of the effective mode area in all cases. Thus by an additional micro-adjustment of this design parameter- d_2 we can obtain remarkable flat dispersion with low value, while at the same time we can engineer the effective mode area to have a large value. It is worth to notice that for all these groups of design parameters the effect to the modal area is almost the same. Further increment of the effective mode area will result in the multi-mode operation of the proposed fiber. A direct way to increase further the effective mode area, while keeping the single mode operation, is by decreasing the air-hole diameters in the cladding- d , on the expense of increasing the required number of air-hole rings, for compensating the higher leakage losses. Keeping this limitation in mind, the finalized optimum values of the proposed PCF have been derived as follows: $\Lambda=2.8\ \mu\text{m}$, $d/\Lambda=0.4$, $d_1/\Lambda=0.29$, and $d_2/\Lambda=0.31$. With this set of design parameters the newly proposed HF structure has the following performance; flattened chromatic dispersion of $6.3\pm 0.5\ \text{ps/km/nm}$ between $1.45\ \mu\text{m}$ to $1.65\ \mu\text{m}$, and effective mode area as large as $100\ \mu\text{m}^2$ in the same wavelength. The choice of this set of design parameters is not random, since it will additionally have an optimum influence to the leakage loss property of the proposed PCF structure in conjunction to all the other sets of design parameters, as will be demonstrated in the next section. In addition we would like to comment on the obtained chromatic dispersion of about $6.3\ \text{ps/km/nm}$, which may seem somewhat large. A direct way to reduce the value of the group velocity dispersion is by decreasing a little bit the pitch constant Λ , on the expense of decreasing a little bit the obtained effective mode area. Even in such case however, the flatness of the chromatic dispersion remains remarkably flat and in addition the effective mode area has higher value than usual optical fibers.

4. Leakage loss properties of the proposed PCF

A very crucial factor that can ensure the potential use of the proposed large mode area PCF as a platform for transmitting information is apparently that the fiber to be single moded and additionally the total attenuation to be as low as possible. We will concentrate our analysis in these factors, and we will show that indeed our proposed PCF structure has a low leakage loss property, under the choice of the optimized design parameters from the previous section. In Fig. 4 we plot the calculated leakage loss of the fundamental mode (circles), as well as the higher order mode (triangles), as a function of the total number of air-hole rings, and for three different operating wavelengths of $1.45\ \mu\text{m}$ (red color), $1.55\ \mu\text{m}$ (blue color), and $1.65\ \mu\text{m}$ (green color), for (a) the following set of design parameters, $\Lambda=2.8\ \mu\text{m}$, $d/\Lambda=0.35$, $d_1/\Lambda=0.28$, $d_2/\Lambda=0.32$, while the same calculation is repeated in Fig. 4 (b) for the optimized set of the design parameters, $\Lambda=2.8\ \mu\text{m}$, $d/\Lambda=0.4$, $d_1/\Lambda=0.29$, $d_2/\Lambda=0.31$, and in Fig. 4(c) for the following set of design parameters $\Lambda=2.8\ \mu\text{m}$, $d/\Lambda=0.45$, $d_1/\Lambda=0.3$, $d_2/\Lambda=0.305$. From these results we can conclude that the set of design parameters in Fig. 4(b) corresponding to the optimized set of the results in Figs. 3(c) and (d), which produces a low leakage loss of the

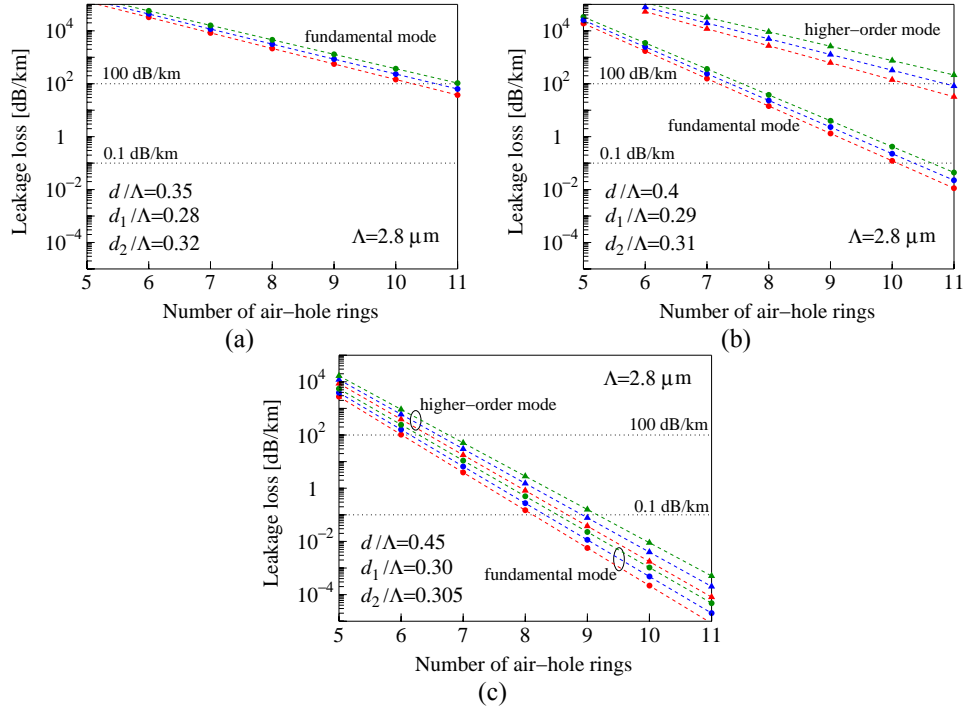


Fig. 4. Calculated leakage loss of the fundamental (circles) as well as of the higher order mode (triangles) in the proposed PCF, at wavelengths of $\lambda = 1.45 \mu\text{m}$ (red color), $\lambda = 1.55 \mu\text{m}$ (blue color), and $\lambda = 1.65 \mu\text{m}$ (green color), as a function of the total number of air-hole rings for (a) the following set of design parameters, $\Lambda = 2.8 \mu\text{m}$, $d/\Lambda = 0.35$, $d_1/\Lambda = 0.28$, and $d_2/\Lambda = 0.32$, (b) the optimized set of design parameters $\Lambda = 2.8 \mu\text{m}$, $d/\Lambda = 0.4$, $d_1/\Lambda = 0.29$, and $d_2/\Lambda = 0.31$, and (c) $\Lambda = 2.8 \mu\text{m}$, $d/\Lambda = 0.45$, $d_1/\Lambda = 0.30$, and $d_2/\Lambda = 0.305$. It is clear that the choice of the set of design parameters in (b) results in a leakage loss of the fundamental mode of three orders of magnitude lower than that of the higher order mode for a total number of eleven air-hole rings.

fundamental mode which is found to be lower than three orders of magnitude (10^{-3}) than that of the higher order mode with the number of air-hole rings to be 11, while on the other hand the results in Fig. 4(c) show that the difference of the leakage loss of the fundamental and the higher order modes is less than one order of magnitude (10^{-1}). It is worth to notice that with the optimized set of design parameters and for a total number of eleven air-hole rings we could achieve a leakage loss of less than 0.03 dB/km at a wavelength of $\lambda=1.55 \mu\text{m}$. In order to study in a more detailed way the mechanism of the electromagnetic field confinement in this type of PCF, in Fig. 5 we examine the electric field distribution for the x -polarized mode in (dB) at fixed wavelength of $\lambda=1.55 \mu\text{m}$ and for fixed cladding air-hole diameters $d/\Lambda=0.4$, for different values of the design parameter d_2/Λ , specifically in Fig. 5(a) for $d_2/\Lambda=0.4$ with corresponding effective mode area of $35 \mu\text{m}^2$, (b) $d_2/\Lambda=0.34$ with an effective mode area of $55 \mu\text{m}^2$, and (c) $d_2/\Lambda=0.31$ with effective mode area of $100 \mu\text{m}^2$. As a conclusion we can say that the effect of the design parameter d_2/Λ to the enlargement of the effective mode area is dominant. In addition we can see that as soon as the effective mode area takes higher values the light tends to be confined in a larger area, and therefore is strongly enhanced into the cladding. The proposed PCF architecture operates as an effectively single mode fiber in the S+C+L telecommunication band, because the calculated leakage loss of the higher order mode was found to be larger than about 100 dB/km in the C+L telecommunication window, while at the beginning of the S-band the calculated value is 32 dB/km. At this point we would like to

address a possible limitation of our proposed PCF structure associated with the existence of the additional air-holes in the central region of the fiber. The inclusion of these air-holes is expected to give rise to an additional loss mechanism, known as scattering loss [6]. This additional loss mechanism is unavoidable in this type of PCF and surely will affect the overall loss performance of the proposed structure. The theoretical estimation of the scattering loss level is quite a difficult task and we believe that only experimental results can show the real picture concerning this loss mechanism.

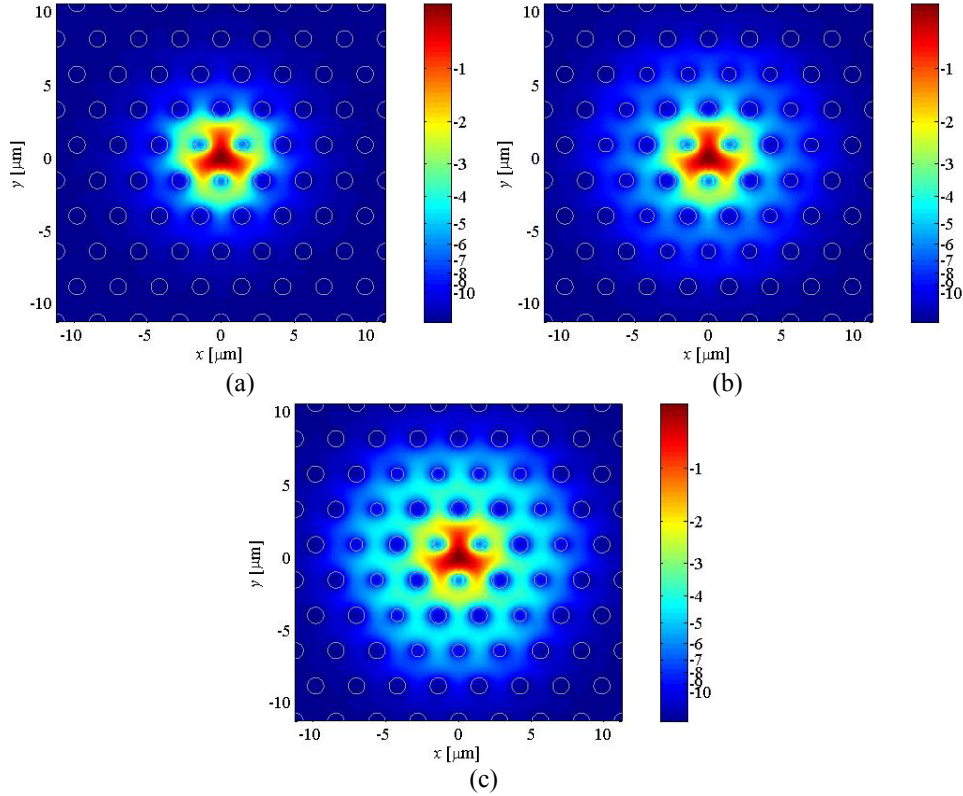


Fig. 5. Normalized electric field distribution of the x-polarized mode in dB at a wavelength of $\lambda = 1.55 \mu\text{m}$, for (a) $d_2/\Lambda = 0.4$ (effective mode area of $35 \mu\text{m}^2$), (b) $d_2/\Lambda = 0.34$ (effective mode area of $55 \mu\text{m}^2$), (c) $d_2/\Lambda = 0.31$ (effective mode area of $100 \mu\text{m}^2$), while the other parameters were fixed at values of $d/\Lambda = 0.4$, and $d_1/\Lambda = 0.29$. Notice that once the effective mode area increases the light confinement is strongly enhanced into the cladding.

5. Feasibility and compatibility of the proposed PCF with conventional fibers

Once we proposed a new device concept it is very important to examine the feasibility and the compatibility of the proposed PCF structure with other conventional optical fiber components. This study is very important in justifying whether our proposed PCF is compatible with other optical cables and can characterize the robustness and/or identify possible flaws during bending operation or during splicing mode. Therefore we concentrate our investigation to characterize the proposed fiber in splicing as well as under bending operation. For this purpose in Fig. 6(a) we plot the calculated bending loss (dB/km) of our PCF structure as a function of the bending radius (cm) at a fixed operational wavelength of $\lambda=1.55 \mu\text{m}$. For calculation of the macro-bending induced loss we employ the tilted index model described

recently in [17]. From the results in Fig. 6(a) we can see that even under a drastic bending operation (for bending radii around 3 cm), the corresponding bending losses remain less than 0.1 dB/km, a result which shows that the proposed PCF doesn't suffer much from macro-bending losses. This observation was actually expected, since the difference between the effective cladding index and the effective index of the fundamental core mode of our proposed PCF, is larger than that of the conventional single mode fibers (SMFs), and this results in the reduction of the bending losses. To justify the compatibility with standard SMFs in Fig. 6(b) we plot the calculated splice loss between the proposed PCF structure and a standard SMF having core radius of 4.8 μm and index difference of 0.3% by adapting the method proposed in [18]. From this analysis we can see that the splice losses remain in a relative low level of about 0.6 dB. As a conclusion we can fairly say that the proposed PCF does not have serious integration issues when splicing to standard SMFs.

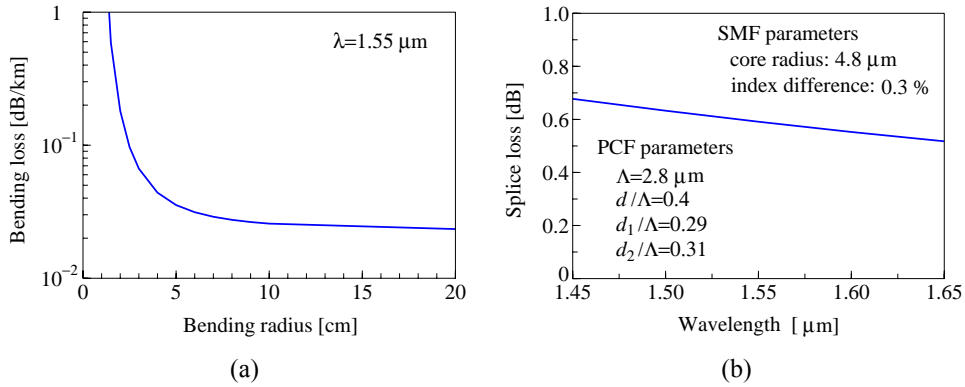


Fig. 6. (a) Calculated bending loss of the proposed PCF with eleven air-hole rings, as a function of the bending radius at fixed operational wavelength of $\lambda = 1.55 \mu\text{m}$ for the optimized design parameters, $\Lambda = 2.8 \mu\text{m}$, $d/\Lambda = 0.4$, $d_1/\Lambda = 0.29$, $d_2/\Lambda = 0.31$, (b) splice losses between the proposed PCF and a standard single mode fiber (SMF) with core radius 4.8 μm and index difference 0.3%. It is evident from these results that the bending losses remain in a lower level compared to standard SMFs, while the splice losses also remain in a relatively low level of about 0.6 dB.

6. Sensitivity analysis of structural disorders to the PCF performance

In the previous sections we have theoretically demonstrated that a PCF having exceptional chromatic dispersion flatness, as well as large effective mode area and low leakage losses in the S+C+L telecommunication band, could be realized using the intriguing approach of incorporating artificial defects into the core and the cladding of a PCF. A crucial question arises however regarding the inevitable imprecision introduced during the fabrication process of such a PCF in the design space variables, which will affect the final performance of the fiber. In order to investigate how such structural disorders affect the overall performance of the proposed PCF architecture, we have performed sensitivity analysis regarding the impact of the fluctuation of the design parameters to certain quantities related to the PCF performance, such as the effective mode area and the chromatic dispersion. Before proceeding we need to identify at the first stage which of the design parameters will have a dominant effect during their possible fluctuations to the above mentioned quantities. Recently it has been pointed out by many research groups [19], that PCFs can demonstrate high lattice uniformity, meaning that the pitch constant- Λ as a design parameter can be considered fairly constant along the PCF cladding. Also for maintaining the effective single mode operation, the air-hole diameters in the cladding- d of the fiber must be kept within very low tolerances. Experimentally it has

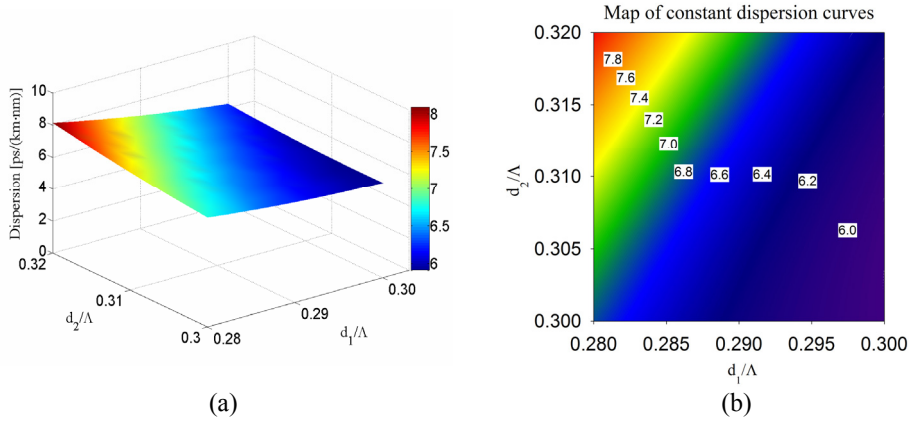


Fig. 7. Sensitivity performance of the chromatic dispersion at a wavelength of $1.55 \mu\text{m}$ as a function of the design parameter space formed by the variables d_1/Λ and d_2/Λ , (a) a three-dimensional plot and (b) a contour map of constant dispersion curves. It is evident from these graphs that the variation to both structural imperfections is linear. In addition we can see that the dynamic rate of change of the chromatic dispersion remains within a $\pm 0.5 \text{ ps/km/nm}$ of its nominal optimized value and therefore we can fairly say that the chromatic dispersion is insensitive to both structural fluctuations.

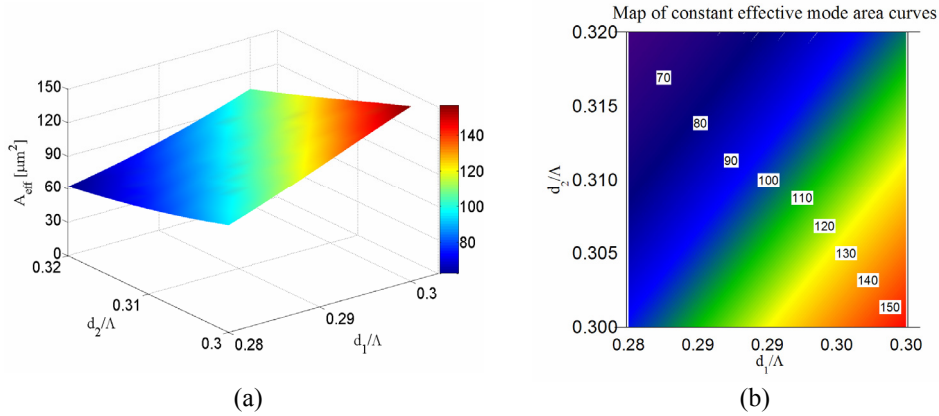


Fig. 8. Sensitivity performance of the effective mode area at a wavelength of $1.55 \mu\text{m}$ as a function of the design parameter space formed by the variables d_1/Λ and d_2/Λ , for (a) a three-dimensional plot and (b) a contour map of constant effective mode area curves. It is evident from these graphs that the variation to both structural imperfections is linear. In addition we can see that the dynamic rate of change of the effective mode area is more sensitive to the variations of the structural parameter d_2/Λ and less sensitive to the fluctuations of the parameter d_1/Λ .

been demonstrated that this is partly true. So at this stage we can fairly say that the critical parameters which their variations may affect drastically the PCF performance are the air-hole diameters in the defected ring- d_2 and the defected air-hole diameters in the core- d_1 . So we will focus our sensitivity analysis on these parameters. Furthermore we have to estimate the rate at which the tolerances may occur in a real design. Following the fabrication data in [20] we see that acceptable tolerances during fabrication did not exceed $\pm 2\%$. So in our sensitivity modeling we assume that the mean absolute value of the design parameters d_1 and d_2 remains within a tolerance of $\pm 2\%$ around their nominal values. In order to understand how this level

of structural fluctuation affects the chromatic dispersion, in Fig. 7(a) we plot in a three-dimensional graph the variation of the calculated chromatic dispersion at a wavelength of 1.55 μm over the two-dimensional space formed by the design parameters, d_1/Λ and d_2/Λ , while Fig. 7(b) shows the map of constant dispersion curves. From the results in Figs. 7(a) and (b) we can conclude at first that the chromatic dispersion changes in a linear fashion with respect to the design parameters d_1/Λ and d_2/Λ . In addition we can determine that the dynamic change of the chromatic dispersion remains within a range of ± 0.5 ps/km/nm from its nominal optimized value, a fact that supports the conclusion that indeed the proposed PCF structure produces a chromatic dispersion profile which is insensitive to the structural variations.

Next we focus our sensitivity calculations to the effective mode area. With respect to the critical design parameters d_1/Λ and d_2/Λ in Fig. 8(a), we plot the effective mode area fluctuation at a wavelength of 1.55 μm as a function of the design parameters, d_1/Λ and d_2/Λ , while Fig. 8(b) shows the map of constant effective mode area curves. From the resulting behavior we can clearly see that the effective mode area changes almost linearly as a function of the design parameters. In this case however we observe that as soon as the structural variations of the design parameter- d_2 significantly increase from its nominal value, the dynamic behavior of the effective mode area will deviate from its linear behavior in a quadratic fashion. The quadratic behavior of the effective mode area for larger values of the tolerance was confirmed by fitting quadratic functions to the calculated by the FEM solver effective mode curves. On the other hand the effect of the structural disorders of the design parameter- d_1 can be considered negligible. As a conclusion we can say that regarding the dynamic rate of change of the effective mode area the design parameter- d_2 has to be kept at low tolerances if we want our design to be robust in terms of information transmission. This result is actually something that we expected to observe, since the results in Figs. 5(a)-(c) suggest that the optical field enhancement into the cladding of the proposed PCF associated with the possibility of the effective mode area enlargement is indeed sensitive to the size of the air-holes in the defected ring.

As a general conclusion of this section, we have estimated the impact of the structural tolerances to important parameters of the PCF's performance, such as the effective mode area and the chromatic dispersion. We showed that the chromatic dispersion flatness of the proposed PCF architecture seems insensitive to possible variations for both design parameters d_1/Λ and d_2/Λ , while on the other hand the effective mode area of the proposed PCF seems to be sensitive only to the structural tolerances of the air-hole diameters in defected ring in the cladding.

7. Conclusions

To summarize this paper we have demonstrated an outstanding approach for realizing PCFs with flat chromatic dispersion, large effective mode area, and low leakage losses. The design principle is based on a novel idea of incorporating various types of artificial defects such as a defected air-hole ring in the cladding, and additional defected air-holes in the core of the fiber. Extensive numerical simulations have been performed from which we conclude that this novel type of PCF is suitable for applications in reconfigurable optical transmission systems or as an information platform in wide-band high speed data transmission systems. Fabrication of the proposed PCF topology and experimental verification of our numerical results is a technological challenge, and the realization of our PCF structure remains an open task. Sensitivity analysis showed that our proposed structure results in a robust design and possible structural disorders may affect the overall response of the PCF, but in an acceptable way for most practical applications. The continues improvement of the fabrication technology of PCFs is expected to reduce further the total attenuation to the level of the conventional optical fiber, and further regulate additional loss mechanisms such as scattering losses from the defected air-holes in the core of the fiber, thus making our proposed PCF an ideal candidate as a platform for transmitting information in high speed transmission systems. We believe that the

inclusion of artificially-defected air-hole rings in the cladding as well as in the core of PCFs can bring considerably freedom in designing various types of PCFs having exceptional propagation characteristics. To this end, the inclusion of artificially defected air-holes in various types of PCFs is currently an active research topic in our group.